$\mathcal{H}_\infty$ Feedback Control for signal tracking on a 4 poster test rig in the Automotive Industry

J.De Cuyper(1), **J. Swevers**(2), **M. Verhaegen**(3), **P.Sas**(2)
(1) LMS International, Interleuvenlaan 68, 3001 Leuven, Belgium
(2) Katholieke Universiteit Leuven, Depart. of Mechanical Eng., Celestijenlaan 300B, 3001 Leuven, Belgium
(3) University of Twente, Faculty of Applied Physics, Meas. & System Eng., P.O.Box 217, Drienerlolaan 5, NL -7500/7522 AE/NB Enschede
e-mail : joris.decuyper@lms.be

Abstract

This paper discusses the design of a $\mathcal{H}_\infty$ control system. The controller is validated on 1 axis of an industrial hydraulic test rig which is used in the automotive industry for vibration comfort evaluations of new vehicle prototypes. The designed $\mathcal{H}_\infty$ controller is a SISO (Single Input Single Output) feedback controller and is used in combination with an industrial available feed-forward controller. The experimental results show that the total controller (feed-forward + $\mathcal{H}_\infty$ feedback) reduces the tracking error compared to the feed-forward controller only. Future work will concentrate on the extension towards the MIMO (Multiple Input Multiple Output) case.

1. Introduction

The motivation for this research comes from the automotive industry where car manufacturers imitate road test drives on multi axial hydraulic test rigs (see figure 1). The goal is to drive the hydraulic shakers of the test rig in order to excite the car such that signals measured on the car during one test drive (called target signals), are reproduced on the test rig. Currently existing software packages like LMS International's 'Time Waveform Replication' [9], control test rigs with an iterative off-line control algorithm, as explained in more detail in section 2.. This industrial available controller can be considered as a feed-forward controller. Controlling the test rigs in real-time, by closing the loop with a feedback controller, can improve the accuracy and speed of the test rig simulations substantially. This paper presents the design and validation results of such a real-time feedback controller.

Various researchers already reported different control techniques to improve the classical iterative off-line control technique. Peng and Mianzo [7] describe an LQ and $\mathcal{H}_\infty$ approach for the control of a durability simulator. De Cuyper et alii [3] describe the application of a LQ and pole placement feedback controller on a laboratory set-up. In his PhD disseration Raath [1] suggests to use time domain models instead of the classically used frequency domain models.

During the replication of target signals on hydraulic test rigs, physical limitations of the actuators and the sensors impose limits on the frequency band which can be controlled. This suggests for the feedback controller design to put emphasis on this frequency band as well. Therefore, this paper proposes an $\mathcal{H}_\infty$ control design approach, since $\mathcal{H}_\infty$ control allows explicitly to specify performance and robust stability criteria within a certain frequency band of interest.

The paper is structured as follows. Section 2. describes in more detail the state-of-the-art multi axial test rig control algorithms. Section 3. explains the basic concepts of $\mathcal{H}_\infty$ control which are relevant to this research and how the $\mathcal{H}_\infty$ controller is combined with the industrial available feed-forward controller. Section 4. continues with a description of the experimental set-up. Section 5. explains how the system was identified and section 6. highlights the design of the $\mathcal{H}_\infty$ controller based on the identified model. Section 7. shows the experimental results and section 8. presents the main conclusions.

2. Controlling multi axial test rigs: state-of-the-art

2.1 The use of multi axial test rigs

When designing a new vehicle, car manufacturers make extensively use of test drives on public roads

and test tracks. During these test-drives, accelerations, forces and displacements are measured at some specific points of the car. On the one hand, these measurements are indispensable to optimize the design of the car for aspects such as durability and comfort. On the other hand, test drives on the road are very expensive and uncomfortable for the driver who has to drive for hours and hours on often severe roads. Therefore, test drives are replaced as much as possible by simulations on a multi axial test rig in a test lab. The multi axial test rig consists of hydraulic shakers, which excite the car such that the responses measured during one test drive on the road are replicated as accurately as possible in a laboratory environment. The simulation is evaluated by comparing the laboratory measurements with the target signals, i.e. the measurements during the test drive.

The number of shakers of an industrial test rig is minimally equal to 4 - allowing a vertical excitation of the 4 wheels of the car - and can go up to 16 allowing to impose on each wheel axis a displacement (or force) in all 3 directions and a breaking torque. Each of the shakers is controlled by means of a PID controller. Figure 1 shows the industrial test rig with 4 shakers, i.e. a so-called 4 poster, used for the experiments described in this paper.

Figure 1: Experimental set-up: industrial 4 poster test rig

2.2 Controlling multi axial test rigs: solving a multivariable tracking problem

Controlling multi axial test rigs is a multivariable tracking problem. The goal is to calculate appropriate input signals for the system, such that the outputs of the dynamic system match given reference signals. In this case, the dynamic system consists of the complete test rig including PID controllers, shakers and the car, while the reference signals are the target signals measured during the test drive on the road.

Dodds [4] was the first to suggest a frequency domain approach to solve this multivariable tracking problem. Today, different software packages are available based on this approach, like for example LMS International's 'Time Waveform Replication' [9]. Basically, the required inputs (also called the 'drives') are calculated in the frequency domain by multiplying the Fast Fourier Transform of the targets with the inverse of a measured Frequency Response Function (FRF) model of the system. Because of non-linearities, model inaccuracies and external disturbances, this off-line calculation leads to an iterative procedure in which the errors, i.e. the differences between the measured signals in the test lab and the target signals, are minimized. The complete iterative drive calculation procedure is explained in more detail in [8] and [2].

As already mentioned, the calculation of the drives is currently an off-line feedback process, meaning that the measured outputs are fed back to the computer only when a complete acquisition has been done. Feeding back the output signals in real-time, by adding a feedback controller can improve the drive calculation procedure substantially. This paper presents the design and experimental validation of a $\mathcal{H}_\infty$ feedback controller meant to reduce the tracking error on the acceleration of the front-left wheel axle of the car mounted on the rig.

3. $\mathcal{H}_\infty$ control: basic concepts

A tutorial introduction to $\mathcal{H}_\infty$ control is given in [6]. A more complete overview of $\mathcal{H}_\infty$ control techniques, how they can be used in a practical control problem and the mathematical details on $\mathcal{H}_\infty$ control can for example be found in [11] and [12].

This section discusses the basic concepts of $\mathcal{H}_\infty$ control which are relevant to this research.

3.1 Feedback control scheme

Figure 2 shows a 1 DOF feedback control scheme. Note that, for simplicity, disturbances and measurement noise are not considered.

The reference (or target) signals are denoted by r, the input to the controlled system G is u, the output

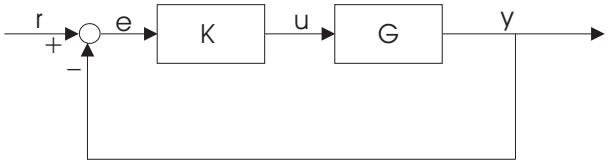

Figure 2: 1 DOF feedback control scheme

of the system is y. The loop is closed by feeding back the tracking error $e = r - y$ to the controller K.

The feedback controller design is based on the control scheme depicted in figure 2. The off-line calculated feed-forward signal is then added afterwards to the here calculated control input.

3.2 Closed-loop transfer functions

It is well known that the closed-loop transfer functions play a primordial role in a controller design. Following closed-loop functions are defined:

- the loop transfer function L:
  $L \equiv GK$
- the sensitivity function S:
  $S \equiv (I + GK)^{-1} = (I + L)^{-1}$
- the complementary sensitivity function T:
  $T \equiv (I + GK)^{-1}GK = (I + L)^{-1}L$

The role which is played by these transfer functions can be seen from the following signal equations, derived directly from figure 2. The signal equations are valid at each frequency, but for simplicity, the dependence of the frequency is not explicitly noted.

$$\begin{aligned} y &= GK(r - y) \\ &= (I + GK)^{-1}GK \quad r \\ &= Tr \end{aligned} \tag{1}$$

and

$$\begin{aligned} e &= r - y \\ &= (I - T)r \\ &= Sr \end{aligned} \tag{2}$$

in which use is made of the identity

$$S + T = I \tag{3}$$

Equation (2) shows that the sensitivity function S is a performance indicator: the lower the sensitivity function, the lower the tracking error and hence, the better the performance. It can be shown (see for example [11]) that, when also taking into account model uncertainties, stability in the presence of multiplicative uncertainty (i.e. robust stability), is obtained when T satisfies $|T| < 1/|w_I|$, where $|w_I|$ is at each frequency equal to the magnitude of the multiplicative uncertainty. So, to obtain a stable closed loop system, T should be made small in frequency regions where the model uncertainty is large. This is also already suggested by equation (1) which indicates that a small T leads to a small output y (and hence a controller with small gains which is unlikely to cause instability).

In this way, a trade-off is made between a small sensitivity function S for good performance and a small complementary sensitivity function T for robust stability. The constraint (3) shows that they cannot be made small simultaneously at the same frequency. Hence, the goal is to design a controller which has a low sensitivity function S in the frequency band of interest and a low complementary sensitivity function T outside this band.

3.3 The term $\mathcal{H}_\infty$

The $\mathcal{H}_\infty$ norm of a transfer function $G(s)$ is the peak value of the largest singular value $\overline{\sigma}$ of $G(j\omega)$ as a function of frequency, that is,

$$\|G(s)\|_\infty \equiv \max_\omega \overline{\sigma}(G(j\omega))$$

In the case of a SISO system, the $\mathcal{H}_\infty$ norm is simply the peak value of $|G(j\omega)|$.

The $\mathcal{H}_\infty$ control methods tries to minimize the $\mathcal{H}_\infty$ norm of some selected closed-loop transfer functions like S or T. By including weighting functions in the $\mathcal{H}_\infty$ control problem, the designer can shape the closed-loop transfer functions according to his specific needs.

3.4 Weighting functions as upper bounds on closed-loop transfer functions

Let $1/|w_P(s)|$ be a desired upper bound on the magnitude of S, where $w_P(s)$ is a weighting function specified by the designer. Then requiring that

$$|S(j\omega)| < 1/|w_P(j\omega)|, \forall\omega,$$

is equivalent to

$$|w_P(j\omega)S(j\omega)| < 1, \forall\omega,$$

or

$$\|w_P(j\omega)S(j\omega)\|_\infty < 1.$$

These equations show how the specification of an upper bound on the sensitivity function S leads to a condition on the $\mathcal{H}_\infty$ norm of the weighted sensitivity $w_P S$.

3.5 Shaping different closed-loop functions: mixed sensitivity

The previous section explained how to specify an upper bound on the sensitivity function S by making use of the performance weighting function w_P. However, since control design is always a trade-off between performance and robust stability, other requirements need to be taken into account; for example the requirement that T is small outside the frequency band of interest.

To combine these requirements on different closed-loop functions, the so-called mixed sensitivity approach [11] can be applied. In this approach, specifying an upper bound $1/|w_P|$ on $|S|$ and an upper bound $1/|w_T|$ on $|T|$, results in the following overall requirement:

$$\|N\|_\infty = \max_\omega \overline{\sigma}(N(j\omega)) < 1; \quad N = \begin{bmatrix} w_P S \\ w_T T \end{bmatrix}$$

After selecting the different closed-loop functions to be taken into account and their weighting functions, the $\mathcal{H}_\infty$ optimal controller is obtained by solving the problem

$$\min_K \|N(K)\|_\infty$$

where K is a stabilizing controller.

3.6 Limitations on the shape of S and T

When specifying the $\mathcal{H}_\infty$ control problem, it is important to note that S and T cannot be given any desired shape as a function of frequency.

The first limitation is given by equation 3,

$$S(j\omega) + T(j\omega) = I, \forall\omega,$$

indicating that S and T cannot be made small simultaneously.

A second limitation is due to the so-called *waterbed formula*, which, for a stable plant and the loop-gain L having at least 2 more poles than zeros, is

$$\int_0^\infty \ln(|S(j\omega)|)d\omega = 0 \qquad (4)$$

This formula shows that the average value of $\ln(|S(j\omega)|)$ is equal to zero, or: when $|S(j\omega)|$ is smalller than 1 ($\ln(|S(j\omega)|) < 0$) in some frequency region, it will be larger than 1 ($\ln(|S(j\omega)|) > 0$) in another region. Hence, peaking of the sensitivity function S can not be avoided.

In the case when the plant contains unstable zeros, the sensitivity function must satisfy an additional integral relationship which further compromises the performance. This additional integral relationship is not discussed here, but, from this integral relationship however, some interesting upper and lower bounds on the achievable bandwidth can be derived [11]: it can be shown that good performance is not possible in the following frequency interval: $[\ \omega_z/2 \quad 2\omega_z\ ]$, with ω_z the frequency of the unstable zero (in rad/s).

3.7 Total control scheme

The control scheme of figure 2 is augmented with an off-line calculated feed-forward signal, which is added to the feedback signal. This leads to the total control scheme depicted in figure 3.

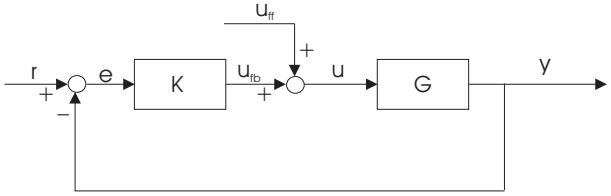

Figure 3: Used control scheme: off-line calculated feed-forward (u_{ff}) + real-time feedback (u_{fb})

As already mentioned, the feed-forward signal is calculated with the industrial available controller, described in more detail in [2]. Note also that the feed-forward signal is calculated based on an open-loop model of the plant G, so not taking into account the feedback loop.

4. Experimental set-up

The experimental set-up consists of the 4 poster test rig shown in figure 1. Wheel pans and belts connected to the vehicle chassis are provided to avoid the vehicle rolling off the rig during the tests. For the feedback experiments described here, only the front-left wheel of the car was excited and one acceleration is measured on the front-left wheel axle, hence

a SISO (Single-Input Single-Output) system is considered. The input of the system is the displacement of the shaker. The hydraulics of the shaker are controlled by a PID controller to ensure that the imposed displacement is indeed realized by the shaker. The frequency band of interest for the experiments lies between 2 and 25 Hz. A sampling frequency of 200 Hz was used.

5. Experimental system identification

An experimental approach is used to identify the SISO system. The car is excited with a periodic noise signal. The spectrum of the signal is flat up to 5 Hz and rolls off for higher frequencies to avoid a too large input amplitude. After calculating the non-parametric Frequency Response Function (FRF) based on a Maximum Likelihood Estimator [10], the state space model is obtained using Non-Linear Least Squares Frequency Domain identification, see also [10]. The best trade-off between model complexity and accuracy was found with a 4th order model.

Figure 4 shows a comparison between the measured FRF and the transfer function derived from the state space model. The figure shows that in the frequency band of interest, i.e. between 2 and 25 Hz, there is a good match between both models.

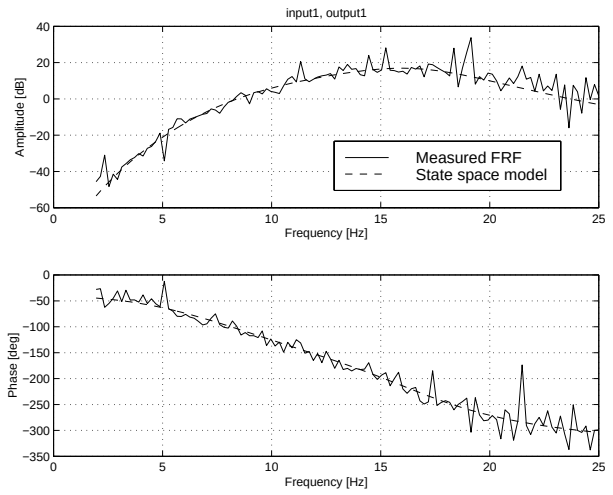

Figure 4: Comparison between non-parametric FRF model with transfer function from state space model

Important from a control point of view, are the poles and zeros of the state space model, which are shown in figure 5. The figure shows that the model contains 1 non-minimum phase zero, at $\zeta = 1.0233$. When using the same discrete-time to continuous-time conversion formulas for zeros as for poles [5], this zero is found to be lying at 0.74 Hz. As explained in section 3.6, this unstable zero will limit the performance in a frequency band between 0.37 Hz and 1.48 Hz. Since this band has no overlap with the frequency band of interest here (i.e. between 2 and 25 Hz), this unstable zero is not expected to cause performance problems.

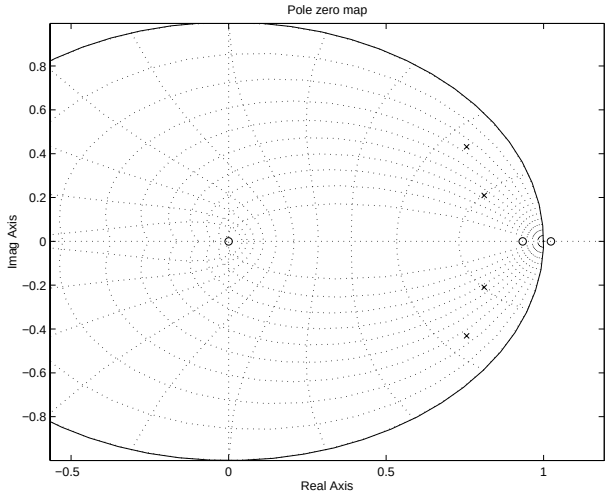

Figure 5: Poles and zeros of the identified state space model

6. $\mathcal{H}_\infty$ Feedback Controller design

The $\mathcal{H}_\infty$ controller is designed making use of the mixed sensitivity approach in which the sensitivity function S and the complementary sensitivity function T are taken into account, see section 3.5.

The weighting functions w_P and w_T provide the tools to specify the trade-off between performance and robustness of the controller. When tight performance bounds are specified, the controller will react strongly but may be unstable on the actual test rig. For safety reasons, the controller design is started with very loose performance bounds, resulting in a controller with very small gains to ensure stability of the controller on the 4 poster. Then, the performance bounds are made more and more tight to gradually increase the performance of the controller. During the experiments, when increasing the controller performance, attention is paid to the amplitude and frequency content of the obtained feedback signal.

Figure 6 shows the amplitude of the inverse of the specified performance weighting function w_P and the obtained sensitivity function S.

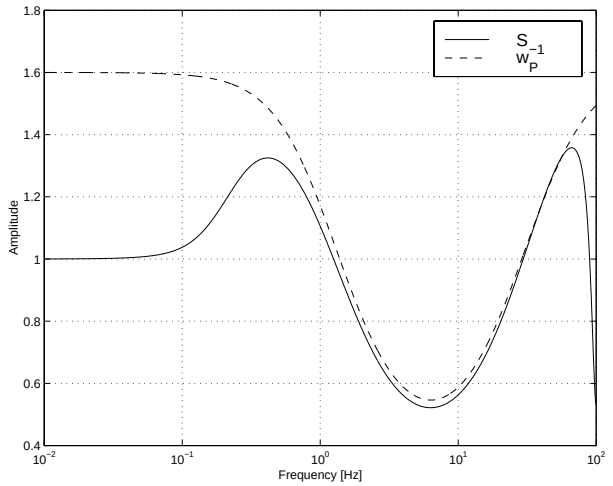

Figure 6: Sensitivity function S and inverse of weighting function w_P

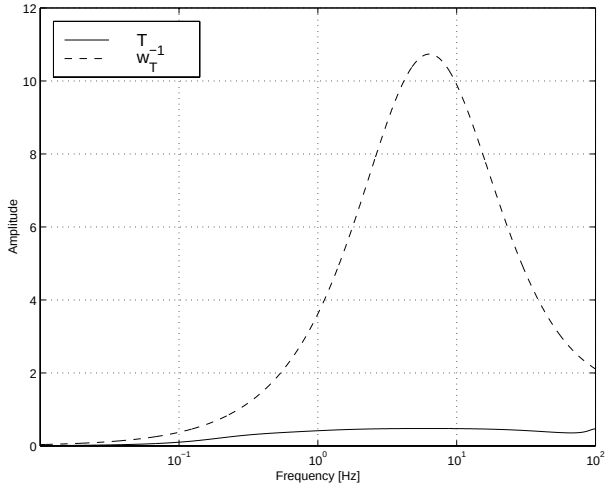

Figure 7: Complementary sensitivity function T and inverse of weighting function w_T

Figure 6 shows that there are two peaks in the sensitivity function which could lead to stability problems of the closed loop system. The experiments showed that the first peak did not lead to any stability problems. The second peak however (around 66 Hz) caused the effect that, the higher the controller performance in the frequency band of interest, the larger the feedback signal around 66 Hz as well. So, to preserve robust stability, the performance could not be further increased.

Figure 7 shows the amplitude of the inverse of the specified weighting function w_T and the obtained complementary sensitivity function T. Note that the bound specified by this weighting function is not tight at all. This weighting function is mainly used to reduce the controller gains at very low frequencies and at the high frequencies.

7. Experimental results

Figure 8 shows the different time signals measured on the front-left wheel axle. A comparison is shown between the reference signal ('target'); the signal obtained when sending out the feed-forward signal only; and the signal obtained with the closed loop system. All signals are filtered between 2 and 25 Hz.

Note that when calculating the feed-forward signal, the target signal has been reduced by 50%. The use of these reduction factors is always used when controlling test rigs; the reason is to guarantee a safe approach: the non-linear behaviour of the rig with vehicle can cause a large mismatch between the model and the actual system which could result in an over-excitation of the test rig when not using a reduction factor. The classical off-line approach then continues by gradually correcting for the remaining difference between measured signals and target signals until satisfactory target reproduction has been obtained.

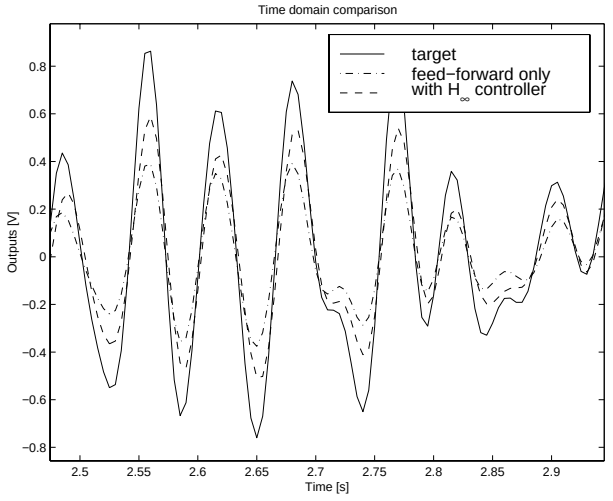

Figure 8: Comparison of target signal with signals measured when using feed-forward only on the one hand and with the $\mathcal{H}_\infty$ controller on the other hand

Figure 8 clearly shows the improvement of the response when making use of the total controller (feed-forward at 50% + $\mathcal{H}_\infty$ controller) with respect to the classically used feed-forward controller at 50%. The shown segment is representative for the complete time signal.

The same result can be represented in the frequency domain by a comparison between the Power

Spectral Densities (PSD's) of the mentioned signals. Figure 9 shows these results. Also in this figure, the improvement is clearly visible.

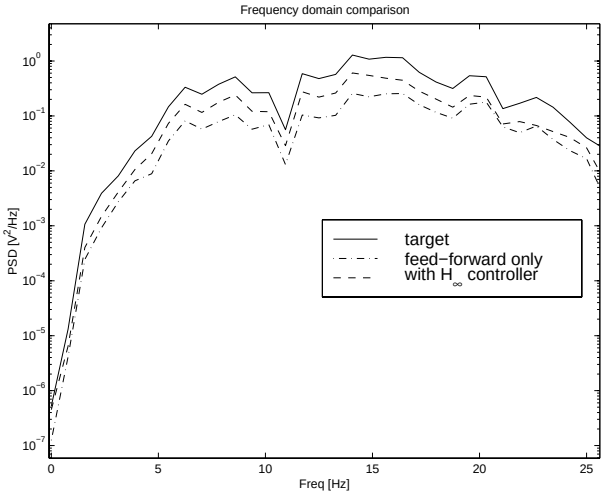

Figure 9: PSD comparison of target signal with signals measured when using feed-forward only on the one hand and with the $\mathcal{H}_\infty$ controller on the other hand

As already mentioned, the limiting factor on the performance of the feedback controller lies in the peak of the sensitivity function at 66 Hz. Further increasing the performance of the controller would result in larger and larger feedback signals or even an unstable closed loop system: the peak in the sensitivity function indicates that the loopgain L is close to the critical point -1 and when the state space model differs significantly from the true system at this frequency, the point -1 can even be encircled resulting in an unstable closed loop system. Identifying a state space model up to higher frequencies would reduce the mismatch between the state space model and the real system and maybe can overcome this limitation.

8. Conclusion

This paper discusses the design of an $\mathcal{H}_\infty$ feedback controller which can be used together with an industrial available feed-forward controller. The application is situated in the automotive industry where the goal is drive multi axial hydraulic test rigs, such that some signals measured during a test drive are reproduced on the test rig.

The $\mathcal{H}_\infty$ controller is designed with the mixed sensitivity approach in which weighting functions on the sensitivity function S and the complementary sensitivity function T are defined. The weighing functions are specified such that the feedback controller is effective in the frequency band of interest, i.e. between 2 and 25 Hz.

The combination of the feed-forward controller and the here designed $\mathcal{H}_\infty$ feedback controller is validated on the front-left corner of a 4 poster test rig (1 input, 1 output). The experimental results show that the proposed control scheme (feed-forward + $\mathcal{H}_\infty$ feedback) improves the response when compared to the classically used feed-forward controller only.

Further research will focus on further increasing the performance of the feedback controller and the extension towards the MIMO case.

9. Acknowledgements

This work was supported by Brite-Euram under contract number BRPR-CT97-0508 and project number BE-97-4186.

The authors also want to thank LTC Ltd., for the granted access to their test facilities and for the technical support during the experiments.

References

[1] A.D.Raath. *Structural dynamic response reconstruction in the time domain*. PhD thesis, Department of Mechanical Engineering, University of Pretoria, 1992.

[2] J. De Cuyper, D. Coppens, C. Liefooghe, J. Swevers, and M. Verhaegen. Advanced Drive File Development methods for improved Service Load Simulation on Multi Axial Durability Test rigs. *Proc. of the Int. Acoustics and Vibration Asia Conference*, pages 339–354, November 11-13 1998.

[3] J. De Cuyper, H. De Keersmaecker, J. Swevers, and D. Coppens. Design of a Multivariable Feedback Control System to drive Durability Test Rigs in the Automotive Industry. *Proceedings of the European Control Conference*, 1999.

[4] C.J. Dodds. *The Response of Vehicle Components to Random Road Surface Undulations*. PhD thesis, Department of Mechanical Engineering, University of Glasgow, 1972.

[5] G.F.Franklin, J.D. Powell, and M.L.Workman. *Digital Control of Dynamic Systems*. Addison Wesley, 2nd edition, 1992.

[6] H.Kwakernaak. Robust Control and $\mathcal{H}_\infty$-Optimization - Tutorial Paper. *Automatica*, 29(2):255–273, 1993.

[7] H.Peng and L.Mianzo. LQ and $\mathcal{H}_\infty$ Preview Control for a Durability Simulator. *Proceedings of the American Control Conference 1997*, 1997. I-97123A.

[8] C. Liefooghe, Gerber, and Haltman. Optimisation of drive comfort of a car by means of a road simulation approach. *Proc. of the 1995 Noise and Vibration Conference*, 1:345–356, 1995.

[9] N. *CADA-X Time Waveform Replication. User Manual*. LMS International, 1998.

[10] J. Schoukens and R. Pintelon. *Identification of Linear Systems. A practical guideline to accurate modeling*. Pergamon Press, 1991.

[11] S. Skogestad and I. Postlethwaite. *Multivariable Feedback Control: Analysis and Design*. J. Wiley, Chichester, 1996.

[12] K. Zhou, J.C.Doyle, and K. Glover. *Robust and Optimal Control*. Prentice-Hall, Upper Saddle River, 1996.